Intramolecular Proton-Transfer Reactions in a Membrane-Bound Proton Pump: The Effect of pH on the Peroxy to Ferryl Transition in Cytochrome *c* Oxidase[†,⊥]

Andreas Namslauer, Anna Aagaard,[‡,§] Andromachi Katsonouri,[§,||] and Peter Brzezinski*

Department of Biochemistry and Biophysics, The Arrhenius Laboratories for Natural Sciences, Stockholm University, SE-106 91 Stockholm, Sweden.

Received July 26, 2002; Revised Manuscript Received December 13, 2002

ABSTRACT: In the membrane-bound redox-driven proton pump cytochrome *c* oxidase, electron- and proton-transfer reactions must be coupled, which requires controlled modulation of the kinetic and/or thermodynamic properties of proton-transfer reactions through the membrane-spanning part of the protein. In this study we have investigated proton-transfer reactions through a pathway that is used for the transfer of both substrate and pumped protons in cytochrome *c* oxidase from *Rhodobacter sphaeroides*. Specifically, we focus on the formation of the so-called F intermediate, which is rate limited by an internal proton-transfer reaction from a possible branching point in the pathway, at a glutamic-acid residue (E(I-286)), to the binuclear center. We have also studied the reprotonation of E(I-286) from the bulk solution. Evaluation of the data in terms of a model presented in this work gives a rate of internal proton transfer from E(I-286) to the proton acceptor at the catalytic site of $1.1 \cdot 10^4$ s^{-1}. The apparent pK_a of the donor (E(I-286)), determined from the pH dependence of the F-formation kinetics, was found to be 9.4, while the pK_a of the proton acceptor at the catalytic site is likely to be ≥2.5 pH units higher. In the pH range up to pH 10 the proton equilibrium between the bulk solution and E(I-286) was much faster than 10^4 s^{-1}, while in the pH range above pH 10 the proton uptake from solution is rate limiting for the overall reaction. The apparent second-order rate constant for proton transfer from the bulk solution to E(I-286) is $>10^{13}$ M^{-1} s^{-1}, which indicates that the proton uptake is assisted by a local buffer consisting of protonatable residues at the protein surface.

The kinetic and thermodynamic properties of intramolecular proton-transfer reactions are important characteristics of a redox-driven proton pump such as cytochrome *c* oxidase. Numerous studies of the pH dependence of the steady-state kinetics of this enzyme have been performed (e.g., ref *1*). However, even though important information can be deduced from such studies, the information about specific reaction steps (e.g., the pK_as of protonatable groups involved) is limited because in many cases the apparent pK_as obtained from the pH dependence of the steady-state parameters are not the true pK_as of specific groups (see, e.g., ref *2*). In addition, even if a specific reaction is investigated in the measurement of the steady-state activity, information is often provided only about the rate-limiting step.

In cases in which the pH dependence of the kinetics and extent of a specific proton-transfer reaction are measured directly, the relevant pK_a values of groups involved in the reaction can often be extracted from the experimental data. Such investigations are particularly important for the understanding of the machinery by which proton pumping is controlled because this machinery may require that the pK_as of the groups involved change during the transitions between different intermediate states of the reaction cycle. This paper is focused on the kinetics of intramolecular proton-transfer reactions, relevant for the understanding of the function of cytochrome *c* oxidase.

The pH dependencies of the rates of specific reaction steps during oxygen reduction in the bovine heart cytochrome *c* oxidase have been presented before (*3*, *4*). In this study we have investigated both the extents and rates of a reaction step that is associated with an internal proton-transfer reaction in the *Rhodobacter (R.) sphaeroides* enzyme and the reprotonation of the internal group from the bulk solution. The results are discussed in the context of information about the structure of the enzyme that we have today and our current knowledge of the mechanism of the enzyme that have emerged during the past few years from studies of the function of different mutant enzyme forms.

Cytochrome *c* oxidase is a membrane-bound enzyme that catalyzes the single-electron oxidation of four molecules of cytochrome *c* and the four-electron reduction of O_2 to water (for review, see refs *5* and *6*). Electrons are first transferred from the water-soluble cytochrome *c* to the primary acceptor copper A, Cu_A.[1] The electron is then transferred consecutively to heme *a* and to the binuclear center which consists of heme a_3 and Cu_B. In the reduced state, heme a_3 binds O_2 which is progressively reduced to water. This process involves the uptake of four (substrate) protons from the

[†] These studies were supported by grants from The Swedish Research Council (VR), The Swedish Foundation for International Cooperation in Research and Higher Education (STINT), The Swedish Cancer Society, and the Human Frontier Science Program (HFSP).

* Corresponding author. Phone: (+46)-8-163280. Fax: (+46)-8-153679. E-mail: peterb@dbb.su.se.

[‡] Present address: University of Queensland, Brisbane, Australia.

[§] These authors have contributed equally to the presented work.

[||] Present address: University of Cyprus, Cyprus.

[⊥] Dedicated to the memory of Eraldo Antonini, prematurely deceased 20 years ago, on March 19, 1983.

10.1021/bi026524o CCC: $25.00
Published on Web 01/24/2003

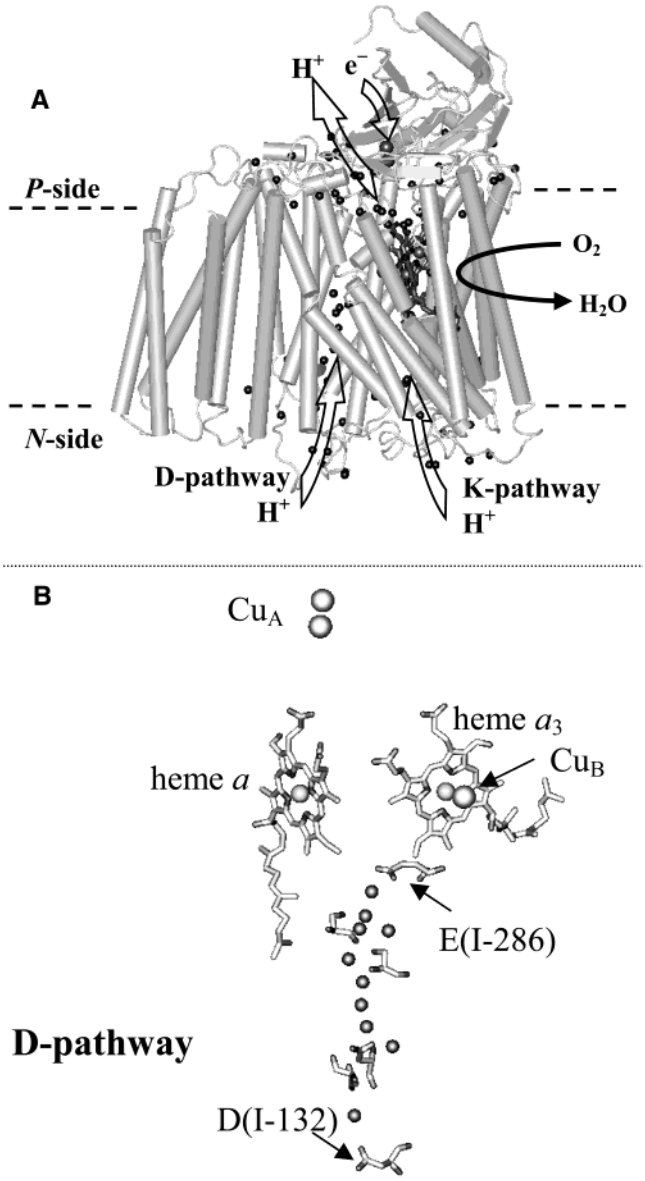

FIGURE 1: (A) The structure of cytochrome *c* oxidase from *R. sphaeroides*. The enzyme catalyzes the oxidation of cytochrome *c* and reduction of O_2 to water. During the process, eight protons (four "substrate" and four "pumped") are taken up from the *N*-side of the membrane, and four protons are released to the *P*-side. (B) The structure of the D-proton-transfer pathway and the redox-active cofactors. The cytochrome *c* oxidase structure is that of the *R. sphaeroides* enzyme (*48*). The picture was prepared using Visual Molecular Dynamic Software (*52*).

negative (N) side of the membrane. In addition, on average one proton per electron is pumped from the N-side to the positive (P) side, across the membrane (see Figure 1A).

The partial reaction steps of the reaction of the fully reduced enzyme with O_2 can be investigated using the so-called flow-flash technique (for review, see refs *7* and *8*). This methodology is based on the ability of reduced heme a_3 to bind CO, thus blocking the O_2 binding site. Consequently, when the fully reduced-CO complex of the enzyme is mixed with O_2, the reaction rate is limited by CO dissociation, which in the enzyme from *R. sphaeroides* displays a time constant of ~30 s. A short time (<1 s) after mixing, CO is dissociated from the enzyme by means of a laser flash, which allows O_2 to bind (see Figure 2). Initially,

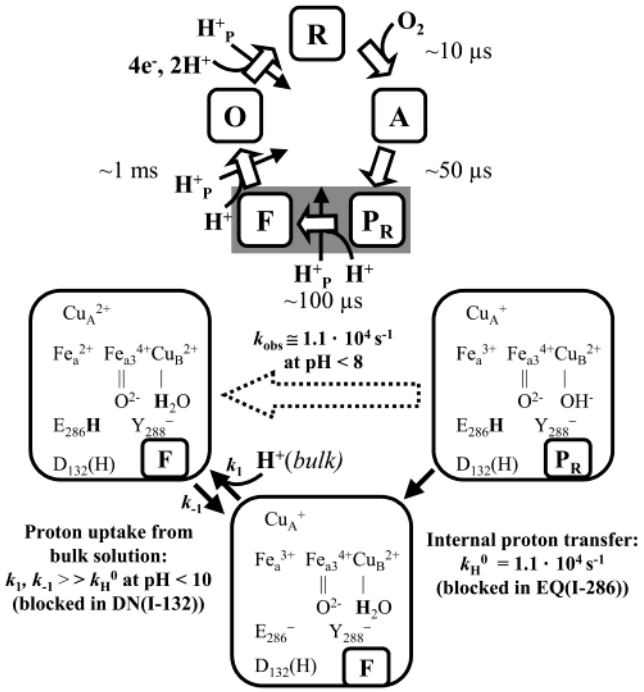

FIGURE 2: A simplified scheme showing the reaction cycle of cytochrome *c* oxidase. The fully reduced binuclear center (R) binds oxygen forming the ferrous-oxy complex (A). After binding of O_2, the O−O bond is broken concomitantly with electron transfer from heme *a* to the binuclear center forming intermediate P_R. Next, the ferryl intermediate, F, is formed at the binuclear center. Finally, the fourth electron is transferred to the binuclear center and another proton is taken up from the bulk solution, forming the fully oxidized enzyme (O). A more detailed view of the $P_R \rightarrow F$ transition is shown in the reaction scheme below the reaction cycle (where Fe_a and Fe_{a3} are the iron ions at heme *a* and heme a_3, respectively). The rate of the $P_R \rightarrow F$ transition at the binuclear center is determined by intramolecular proton-transfer from E(I-286) to the acceptor site at the binuclear center (OH^- bound to Cu_B), followed by rapid reprotonation of E(I-286) from the bulk solution and electron transfer from Cu_A to heme *a*. The Tyr in the catalytic site is Y(I-288), which presumably donates a proton to O_2 during formation of intermediate P. Protons are pumped during the $P_R \rightarrow F$ and $F \rightarrow O$ transitions and also during reduction of the oxidized enzyme (marked as H^+_P, the number of pumped protons is not indicated). Two water molecules are released during each cycle (not shown).

the heme a_3−oxy complex (called A) is formed with a time constant of ~10 μs (at 1 mM O_2) (*3*, *9*). Binding of O_2 to the reduced heme a_3 is followed by electron transfer from heme *a* to the binuclear center and breaking of the O−O bond with a time constant of ~50 μs. The transient intermediate formed at the binuclear center is called P_R (for historical reasons this intermediate is called "peroxy" even though there is a ferryl bound at heme a_3, see Figure 2) (*10*, see also ref *11*). Its formation rate is not pH-dependent and involves only transfer of an internal proton within the enzyme, presumably from residues located in the immediate

[1] Abbreviations and Definitions: Cu_A, copper A; Cu_B, copper B; binuclear center, heme a_3 and Cu_B; WT, wild type; substrate proton, proton used for reduction of O_2 to H_2O (cf. pumped proton); R, cytochrome *c* oxidase with a fully reduced binuclear center; P_R, the "peroxy" intermediate formed at the binuclear center upon reaction of the fully reduced cytochrome *c* oxidase with O_2; F, "oxo-ferryl" intermediate; O, fully oxidized enzyme; *N*-side, negative side of the membrane; *P*-side, positive side of the membrane; *k*, rate constant; τ, time constant (k^{-1}). Mutant-enzyme nomenclature: D(I-132), aspartic acid of subunit I at position 132; DN(I-132), replacement of D(I-132) by asparagine; LM, dodecyl-β-D-maltoside.

vicinity of the binuclear center (*12*). In other words, there is no net proton uptake from solution on the time scale of P_R formation (*9*, *12*, *13*). Consequently, in state P_R there is one more negative charge at the catalytic site as compared to the other intermediate states of the reaction (see Figure 2).

In the next reaction step, the excess negative charge is neutralized by proton uptake from the bulk solution forming intermediate state F with a time constant of ~100 μs (at neutral pH) (*9*, *13*), concomitant with electron equilibration between Cu_A and heme *a* (*14*, *15*, see also ref *16*). The difference between P_R and F is only the additional proton at the binuclear center (see Figure 2); i.e., the $P_R \rightarrow F$ transition does not involve any additional transfer of electrons to the catalytic site. It has been shown that the formation of intermediate F involves a two-step proton transfer through the D-pathway (Figures 1B and 2), in which rate-limiting proton transfer from E(I-286)[2] to the catalytic site is followed by rapid reprotonation of the group from the bulk solution (*17*−*19*) (described in detail in the Discussion section). Thus, during the $A \rightarrow F$ transition (through P_R), one electron and one proton are transferred to the catalytic site in two distinct, kinetically resolved reaction steps; electron transfer from heme *a* to the catalytic site (formation of P_R, $\tau \cong 50$ μs) is followed by proton uptake from the bulk solution (formation of F, $\tau \cong 100$ μs).

It has been shown that in reaction steps that are associated with proton pumping, the proton uptake takes place through the D-pathway (see, e.g., ref *20*). Hence, the transfer of the substrate proton to the binuclear center must be coupled by a specific mechanism to the translocation of a pumped proton (see ref *21*). Since the proton-transfer reaction from the bulk solution to the catalytic site is rate limited by the internal proton transfer from E(I-286) to the catalytic site, a detailed kinetic investigation of the $P_R \rightarrow F$ transition is important for the understanding of proton pumping in cytochrome *c* oxidase.

In this paper, we present results from experimental studies of the internal proton-transfer reaction from E(I-286) to the catalytic site and the reprotonation of E(I-286) from the bulk solution. Then, we discuss these results in the context of theoretical models and the mechanistic features of proton transfer in cytochrome *c* oxidase.

MATERIALS AND METHODS

Growth of Bacteria and Purification of Cytochrome c Oxidase. *R. sphaeroides* expressing either wild-type or DN(I-132), histidine-tagged, cytochrome *c* oxidase were grown aerobically at 30 °C in shaker incubators. Cytochrome *c* oxidase was purified as described in refs *22* and *23*, with the exception that in the last step the enzyme was eluted from the Ni^{2+}-affinity column with imidazole rather than with histidine. The buffer was exchanged to 0.1 M Hepes, pH 7.4, 0.1% dodecyl-β-D-maltoside (LM), and the enzyme was stored frozen at −80 °C. The DN(I-132) mutant enzyme was constructed as described earlier (*24*).

Preparation of the Fully Reduced CO-Bound Enzyme. The buffer in the wild-type enzyme sample was exchanged for 100 mM KCl, 0.1% LM, pH ~7.5 (no buffer was added at this point, see below) by gel filtration on a PD-10 column (Amersham biosciences) that was preequilibrated with the same solution. The enzyme was diluted to a concentration of ~15 μM. The solution was transferred to an anaerobic cuvette, and the electron mediator phenazine methosulfate (PMS) was added to a concentration of 0.7 μM. The air in the cuvette was exchanged for nitrogen on a vacuum/gas line and 2 mM of ascorbate was added to reduce the enzyme. When formation of the fully reduced state was complete, nitrogen was exchanged for CO.

The preparation of fully reduced CO-bound DN(I-132) mutant enzyme was done as with the wild-type enzyme but the enzyme was incubated and reduced in the respective buffer solutions: 100 mM Hepes, pH 7.5; 100 mM CHES, pH 9.4; 100 mM CAPS, pH 10.3, all containing 0.1% LM.

Flow-Flash Experiments. The experimental setup has been described earlier in (*25*). In short, the fully reduced CO-bound enzyme was mixed with an oxygen saturated buffer (ratio 1:5), at the respective pH, in a modified combined stopped-flow/flash-photolysis setup (Applied photophysics, U.K.). After mixing, CO was dissociated by a 7 ns laser flash at 532 nm provided by a frequency-doubled Nd:YAG laser (Brilliant B, Quantel, France). The reactions were followed by recording the absorbance changes at single wavelengths. The cuvette path length was 1.0 cm. To extract the rate constants and extents of formation and decay of the intermediate states, the time-resolved changes in absorbance, measured at different wavelengths, were fitted globally to a multiexponential function using the Pro-K software (Applied photophysics, U.K.).

The flow-flash experiments were performed at 16 different pH values in the range 6−11. The oxygen-saturated buffer consisted of 50 mM Bis-Tris Propane (pK_as of 6.8 and 9.0), 50 mM CAPS (pK_a 10.4), 0.1% LM, and the pH was adjusted by additions of HCl or KOH. For the proton-uptake measurements, instead of buffer, an oxygen-saturated solution of 100 mM KCl, 0.1% LM, supplemented with 48 μM of phenol red (pK_a 7.8) or phenolpthalein (pK_a 10.2) was used. In these cases also the enzyme solution was adjusted to the same pH before the measurement. To determine the number of protons corresponding to a certain absorbance change of the dye, known amounts of HCl were added to the sample, and the corresponding absorbance changes were monitored (*9*).

As a control, wild-type enzyme samples were also prepared (at pH 6 and 10) in which the enzyme was incubated and reduced in the same buffer solution and at the same pH as the respective oxygen buffers. This was done to test whether the proton equilibration of the enzyme with the buffer after mixing was complete before the reaction with oxygen was initiated by the laser flash.

RESULTS

The absorbance changes at 580 (Figure 3), 445, and 605 nm (not shown) were measured after initiation of the reaction of the fully reduced *R. sphaeroides* cytochrome *c* oxidase with O_2 at different pH values. The data were fitted to a function consisting of a sum of three exponentials corresponding to the transitions $A \rightarrow P_R$, $P_R \rightarrow F$, and $F \rightarrow O$. At 580 nm (Figure 4), the unresolved initial step at $t = 0$ is associated with the dissociation of CO from the reduced

[2] If not otherwise indicated, amino acid residues are numbered according to the *R. sphaeroides* cytochrome *c* oxidase sequence.

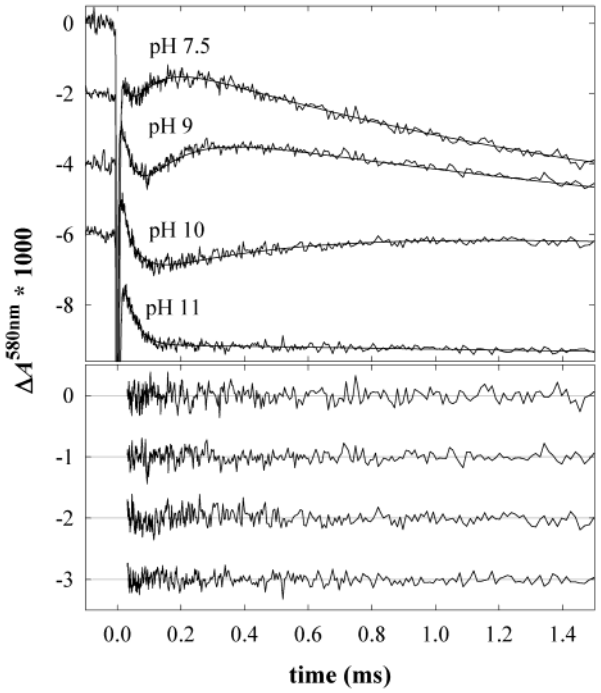

FIGURE 3: Absorbance changes at 580 nm after flash-induced dissociation of CO from the fully reduced wild-type cytochrome *c* oxidase in the presence of O_2. The increase in absorbance from $t \cong 0.1$ ms, seen at pH 7.5, 9, and 10, is associated with formation of the F intermediate. The following decrease in absorbance, seen at pH 7.5 and 9 on this time scale, is associated with the decay of F and formation of the oxidized enzyme (state O). The data at 580 nm, together with data from 445 nm (not shown), were fitted with a sum of three exponentials ($\Delta A(t) = \sum_{i=1}^{3} \Delta A_i(t) \cdot \exp(-k_i t)$, starting at $t = 35$ μs, i.e., after the R to A transition ($k_{R\rightarrow A} \cong 1.3 \cdot 10^5$ s^{-1}). The three components correspond to the A $\rightarrow$ P_R, P_R $\rightarrow$ F, and F $\rightarrow$ O transitions, respectively. Fitting parameters were $k_{A\rightarrow P_R} = 3\pm1\cdot10^4$ s^{-1} (first component in the sum), $\Delta A^{580}_{A\rightarrow P_R} = 4\pm1\cdot10^{-3}$, the rates and amplitudes at 580 nm of the second component corresponding to the $P_R \rightarrow$ F transition are pH-dependent and given in Figure 4, $k_{F\rightarrow O} = 1\cdot10^2 - 1\cdot10^3$ s^{-1}, depending on pH (increases with decreasing pH), $\Delta A^{580}_{F\rightarrow O} = 5\pm1\cdot10^{-3}$. All absorbance changes were scaled to 1 μM reacting enzyme. The fits are presented as solid noise-free lines, and the residuals are shown in the lower panel. Conditions (after mixing): 42 mM Bis-Tris Propane, 42 mM CAPS, 17 mM KCl, 0.1% LM, 400 μM ascorbate, 140 nM PMS, pH as indicated in the graph, 2−3 μM reacting enzyme, 1 mM O_2, $T = 22$ °C. Each trace shown is an average of 5−10 traces at the respective pH value. The traces have been scaled to 1 μM reacting enzyme (the concentrations of reacting enzyme were determined from the CO-photolysis absorbance changes at 445 nm using an absorption coefficient ($\Delta\epsilon$) of $8.9\cdot10^4$ M^{-1}cm^{-1}, (*39*)).

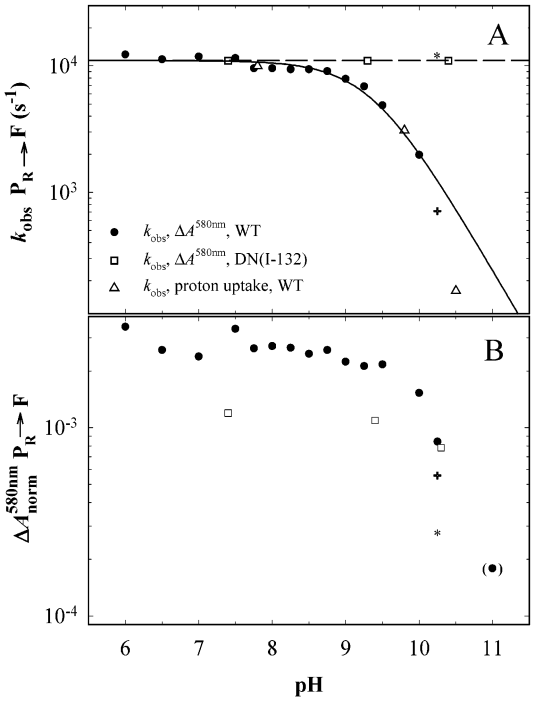

FIGURE 4: The rate (A) and amplitude (B) of F formation measured at 580 nm (see Figures 3 and 6) with the wild-type (●) and DN(I-132) mutant (□) enzymes as a function of pH. At pH 10.3 the formation of F was biphasic with the two rates and amplitudes indicated in the graph (+, *). The rate of the fastest phase of proton uptake (Δ, see Figure 5) is also plotted in (A). At pH 11 the rate of the $P_R \rightarrow$ F transition merges with that of the F $\rightarrow$ O transition. Therefore, we could only determine the amplitude of the rapid component (k_H^0), which is shown in parentheses. The solid line in panel A is a plot of eq 2 using the parameters $pK_a(E) = 9.4$ and $k_H^0 = 1.1\cdot10^4$ s^{-1}. The rate of F-formation in the DN(I-132) mutant enzyme is constant at all measured pH values $k_{OBS} = k_H^0 = 1.1\cdot10^4$ s^{-1}, and the amount of F formed was smaller with the DN(I-132) than with the wild-type enzyme (see Discussion). The absorbance changes have been scaled to 1 μM reacting enzyme (the concentrations of reacting enzyme were determined from the CO-photolysis absorbance changes at 445 nm using a $\Delta\epsilon$ of $8.9\cdot10^4$ M^{-1}cm^{-1}). The rates and amplitudes shown in the graph are obtained from one set of measurements with one enzyme preparation. Each value was determined from a global fit of the kinetic traces at the measured wavelengths where each kinetic trace is an average of 5−10 measurements. The standard deviation from the curve fitting was 10%. The same experiments were done with three different enzyme preparations (results not shown). The standard deviation of the parameters from measurements with different enzyme preparations is given in the text.

enzyme, followed by O_2 binding to heme a_3 (forming state A). The decrease in absorbance with a time constant of 50 μs is associated with the A $\rightarrow$ P_R transition. The following increase in absorbance in the pH 7.5, 9, and 10 traces is attributed to the $P_R \rightarrow$ F transition at the catalytic site. The transition displays a time constant of ~100 μs at pH <8.5. At pH 11 no increase in absorbance after P_R formation was seen (see Discussion). The following decrease in absorbance (of which only the initial part is seen in the pH 7.5 and 9 traces) is associated with decay of the F intermediate to form the oxidized state (O). This transition involves electron transfer from the heme *a*/Cu_A equilibrium to the binuclear center and proton uptake from the bulk solution through the D-pathway. At pH 10 and 11, this decay occurred on a slower time scale and it is not seen in the graph. Figure 4 shows the pH dependence of the observed $P_R \rightarrow$ F transition rate and the amplitude of the 580 nm absorbance increase associated with this transition.

We also investigated the pH dependence of the rate and extent of proton uptake from the bulk solution during the reaction of the wild-type enzyme with O_2 (measured using a pH-sensitive dye). These results provide information about the proton equilibration rate between the bulk solution and the enzyme at different pH values. Figure 5 shows absorbance changes of the pH-sensitive dye phenol red at pH 7.8, monitored at 560 nm, and the dye phenolpthalein at pH 9.8 and 10.5, monitored at 550 nm. At pH 7.8 and 9.8, the fastest phase of proton uptake has the same rate as that of the P_R $\rightarrow$ F transition ($\tau \cong 100$ and 330 μs at pH 7.8 and 9.8, respectively; see also Figure 4A). Two additional phases of

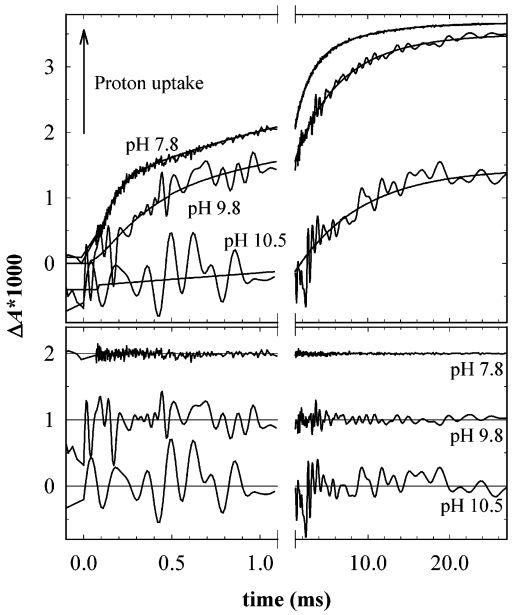

FIGURE 5: Absorbance changes at 560 nm of the dye phenol red (at pH 7.8) and at 550 nm of phenolphthalein (at pH 9.8 and 10.5), associated with proton uptake (absorbance increase) from the bulk solution after flash-induced dissociation of CO from fully reduced wild-type cytochrome *c* oxidase in the presence of O_2. The data at pH 7.8 and 9.8 were fitted with a sum of three exponentials, while the data at pH 10.5 were fitted with one exponential (solid noise-free lines). The residuals are shown in the lower graph. At pH 7.8 and 9.8, absorbance changes were normalized so that length of the arrow in the left upper corner correspond to the uptake of one proton per enzyme molecule. The absorbance change at pH 10.5 is arbitrarily scaled. Conditions: 100 mM KCl, 0.1% LM, 40 μM phenol red or phenolphthalein, 400 μM ascorbate, 140 nM PMS, pH as indicated in the graph, 2−3 μM reacting enzyme, 1 mM O_2, $T = 22$ °C. Each trace shown is an average of 5−10 traces at the respective pH value. At the wavelengths at which measurements were done, the absorbance contribution from the heme groups is very small. To correct for these absorbance changes, signals from buffered samples were subtracted from those of the unbuffered samples.

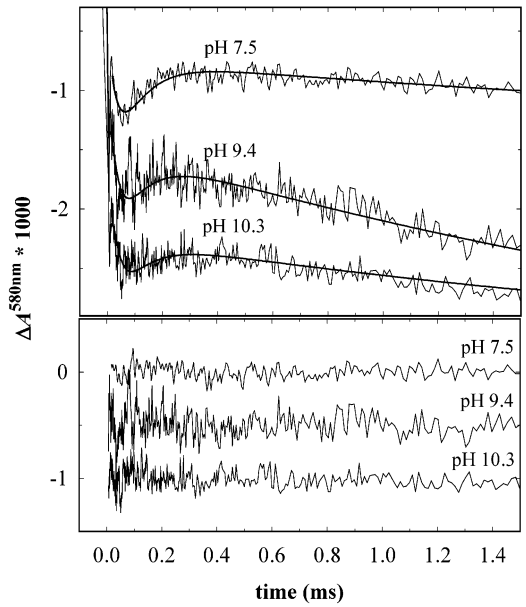

FIGURE 6: Absorbance changes at 580 nm after flash-induced dissociation of CO from fully reduced DN(I-132) mutant cytochrome *c* oxidase in the presence of O_2. The increase in absorbance in the time range ∼50−300 μs, associated with formation of the F intermediate, is smaller than that of the wild-type enzyme (cf. Figure 3 and Figure 4B); see text for details. The absorbance data at 580 and 445 nm (not shown) were fitted with a sum of three exponentials as described in the text and in the figure caption to Figure 3. Fitting parameters were $k_{A\rightarrow P_R} \cong 3\cdot10^4$ s^{-1}, $\Delta A^{580}_{A\rightarrow P_R} = 1.4 \pm 0.1 \times 10^{-3}$, $k_{P_R\rightarrow F} \cong 1.1\cdot10^4$ s^{-1}, and the amplitudes at 580 nm of the second component are given in Figure 4B, $k_{F\rightarrow O} = 1\cdot10^2-1\cdot10^3$ s^{-1}, depending on pH (increases with decreasing pH). A third phase with $k \cong 2.7\cdot10^2$ s^{-1} and amplitudes at 580 nm ranging from 0.7 to $2.4\cdot10^{-3}$ absorbance units was also included. The fits are presented as solid noise-free lines, and the residuals are shown in the lower panel. Conditions: 0.1% LM; 1−2 μM reacting enzyme, 1 mM O_2, 400 μM ascorbate, 140 nM PMS, $T = 22$ °C. Buffers were as follows: pH 7.5, 100 mM Hepes; pH 9.4, 100 mM CHES; pH 10.3, 100 mM CAPS. Each trace shown is an average of 5−10 traces at the respective pH value. All absorbance changes were scaled to 1 μM reacting enzyme (the concentrations of reacting enzyme were determined from the CO-photolysis absorbance changes at 445 nm using a $\Delta\epsilon$ of $8.9\cdot10^4$ M^{-1} cm^{-1}).

proton uptake are seen, one concomitant with the F → O transition and one slower with a time constant of ∼5 and ∼7 ms at pH 7.8 and 9.8, respectively. About 1 H^+ per enzyme were taken up in each of the P_R → F and F → O reaction steps and 0.6 H^+ in the slower phase at both pH values. At pH 10.5 the proton uptake was fitted to one phase with a time constant of ∼7 ms. The extent of this phase could not be determined (see legend of Figure 5).

To investigate whether the pH dye/buffer could assist in proton transfer during F formation at high pH, the reaction at pH ∼10 was studied also in the absence of the dye or buffer. The same rate and extent of F formation were observed without and with the dye/buffer (data not shown).

To investigate the P_R → F transition in a system in which the internal proton-donating group is not reprotonated from the bulk solution on the time scale of the P_R → F transition, we studied the pH dependence of the 580 nm absorbance changes in the DN(I-132) mutant enzyme. In this mutant enzyme, the proton uptake from the bulk solution is blocked at the entrance of the D-pathway, and the F intermediate is formed using the internal proton in the D-pathway (*17*−*19*). Hence, the extent of F formation, as determined from the amplitude of the absorbance increase at 580 nm, reflects the fraction of the protonated internal donor prior to the initiation of the reaction. Figure 6 shows the absorbance changes monitored at 580 nm measured with the DN(I-132) mutant enzyme at three different pH values. It is seen that the rate of F formation is the same at all three pH values ($k \cong 1.1\cdot10^4$ s^{-1}), while the amplitude decreases at increasing pH. The F → O transition rate is limited by the proton uptake from the bulk solution and is slowed by a factor of ∼200 due to removal of D(I-132). There is also a small decrease in absorbance at 580 nm with a time constant of ∼4 ms that follows F-formation (see Discussion).

We also investigated the pH dependence of the P_R → F reaction rate with the bovine heart cytochrome *c* oxidase (data not shown). The pK_a was determined to be ∼8, which is in agreement with published results (*3*, *4*). However, with the bovine enzyme the lowest value at which the rate levels out at high pH is $\sim5\cdot10^3$ s^{-1}, while the experimental data with the *R. sphaeroides* enzyme could be satisfactorily fitted to an equation in which $k_{obs} = 0$ at pH →∞. This difference suggests that in the bovine heart enzyme there is (at least) one more group, which is able to donate a proton to the binuclear center.

DISCUSSION

In this study we have investigated an internal proton-transfer reaction from a protonatable group in the D-pathway to the catalytic site during the $P_R \rightarrow F$ transition in cytochrome *c* oxidase. Because this pathway is also involved in the transfer of pumped protons, information about the kinetics of this reaction step is important for the understanding of the mechanism of proton pumping.

Proton Transfer during the $P_R \rightarrow F$ Transition. Formation of intermediate F from P_R requires protonation of a group at the binuclear center (Figure 2). The replacement of E(I-286) in the D-pathway (see Figure 1B) by its nonprotonatable analogue Gln results in blockage of the catalytic cycle at P_R (*26*−*28*); i.e., the proton needed to form intermediate F is not transferred to the binuclear center in the EQ(I-286) mutant enzyme (*26*). Replacement of E(I-286) by another protonatable residue, Asp, resulted in a slightly slowed F formation (factor of ∼5) (*17*). When proton transfer was blocked further down the pathway, at D(I-132), close to the protein surface, the F intermediate was formed, but the associated proton uptake from solution was impaired (*18*, *19*). Together, these results show that the P_R to F transition can occur using a proton from an internal donor within the D-pathway, without proton uptake from the bulk solution (*17*, *18*). The mechanism was confirmed recently in a study of the effect of Zn^{2+} on the kinetics of specific reaction steps in cytochrome *c* oxidase. The Zn^{2+} ions presumably bind at the protein surface near D(I-132) (there are also other Zn^{2+}-binding sites, *29*), which had as an effect that proton uptake from the bulk solution was impaired, but still F was formed with about the same rate as without Zn^{2+} (*19*). On the basis of the discussion above and taking into account the fact that E(I-286) is the only protonatable amino acid residue "above" D(I-132), we assume that E(I-286) is the proton donor to the binuclear center during the $P_R \rightarrow F$ transition (see Figure 2). This assumption is further supported by results from studies of a double mutant of *R. sphaeroides* enzyme in which E(I-286) "was moved" to another α-helix on the opposite side of the D-pathway. The mutant enzyme was able to reduce O_2 to water and pump protons, but the rate of the $P_R \rightarrow F$ transition was slowed by a factor of 20, and the apparent pK_a associated with the $P_R \rightarrow F$ transition was shifted to <7 (*30*). In addition, results from a recent study (Namslauer et al., unpublished) showed that the apparent pK_a changes upon introduction of an Asp in the vicinity of E(I-286).

On the basis of the above-discussed results, we evaluate the data presented in this study using the following model (see also Appendix and Figure 7):

$$(\text{bulk}) \underset{k_{-1}}{\overset{k_1}{\rightleftharpoons}} E_HC \xrightarrow{k_H^0} EC_H \qquad (1)$$

where (bulk) is the bulk solution (i.e., a proton pool), E is assumed to be E(I-286), and C is the binuclear center. The subscript H indicates a protonated site. In this study C and C_H correspond to states P_R and F, respectively, at the binuclear center. An important assumption of the model is that the proton transfer from E(I-286) to the catalytic site is irreversible, which is discussed in detail below.

The above-discussed results indicate that at neutral pH there is a rapid equilibrium between E(I-286) and the bulk solution, while the internal proton transfer from E(I-286) to the proton acceptor at the binuclear center is slower. According to the model in eq 1, if the equilibrium between the bulk solution and the protonatable group E is much faster than the proton-transfer rate from E_H to C, i.e., $k_1 \gg k_H^0$, one of the terms in eq A3 (see Appendix) vanishes and $[EC_H](t,\text{pH})$ is approximated by a single-exponential function:

$$[EC_H](t,\text{pH}) \cong 1 - \exp(-t \cdot k_{obs}(\text{pH})) \qquad (2a)$$

$$k_{obs}(\text{pH}) = k_H^0 \cdot \alpha_{EH}(\text{pH}) \qquad (2b)$$

$$\alpha_{EH}(\text{pH}) = \frac{1}{1 + 10^{\text{pH}-\text{p}K_a(E)}} \qquad (2c)$$

where α_{EH} is the fraction of group E in the protonated state. This scenario is illustrated in Figure 7A (case 1). In this case the F intermediate (C_H, see above) is formed with the same pH-dependent rate, k_{obs}, in the entire enzyme population (i.e., the amplitude of the absorbance changes associated with formation of F is pH independent). The observed rate (k_{obs}) is determined by the proton-transfer rate from E_H to C (k_H^0) and the fraction protonated E (α_{EH}), where the fraction protonated E is determined by the bulk pH and the pK_a of E. The observed rate of proton uptake from the bulk solution is the same as that of F formation (k_{obs}) even though the intrinsic rate of the proton uptake from the bulk solution to E in itself is much faster.

Internal Proton Transfer in the D-Pathway. In the pH range up to pH ∼10, the absorbance changes associated with formation of F (measured at 580 nm) were found to display a pH-independent amplitude and were found to be monophasic with a rate that decreased with increasing pH (see Figures 3 and 4). This scenario is consistent with the above-discussed limiting case (eq 2). The data could be fitted well to eq 2b,c with a pK_a(E) of 9.4 ± 0.2 and an intramolecular proton-transfer rate from E_H to C, k_H^0, of 1.1 ± 0.2 × 10^4 s^{-1}. (Mean value ± standard deviation, based on results from measurements on three different enzyme preparations. The standard deviation associated with measurements on each preparation was smaller.) It should be noted that at, e.g., pH 10 and 10.3, the protonation fraction of group E is ∼20% and ∼10%, respectively. This means that the pK_a of E can be determined accurately using the measured data up to pH 10 (the data above pH 10 are discussed below).

It is interesting to note that the data fit well with a simple Henderson−Hasselbach titration curve. Groups within proteins often show complicated titration patterns due to interactions with neighboring protonatable groups, as shown, e.g., for cytochrome *c* oxidase (*31*). Thus, the results from this study suggest that the rate of the $P_R \rightarrow F$ transition is determined by the protonation state of a single residue (see also (*32*)).

As pointed out above, an important assumption of the model in eq 1 is that the proton transfer from E(I-286) to the catalytic site is irreversible. This means that the pK_a of the proton acceptor at the catalytic site (in state P_R) is much higher than that of E(I-286). It is reasonable to assume that the protonation reaction at the catalytic site drives the translocation of the pumped proton. Thus, in the absence of an electrochemical potential gradient (i.e., in this study), the

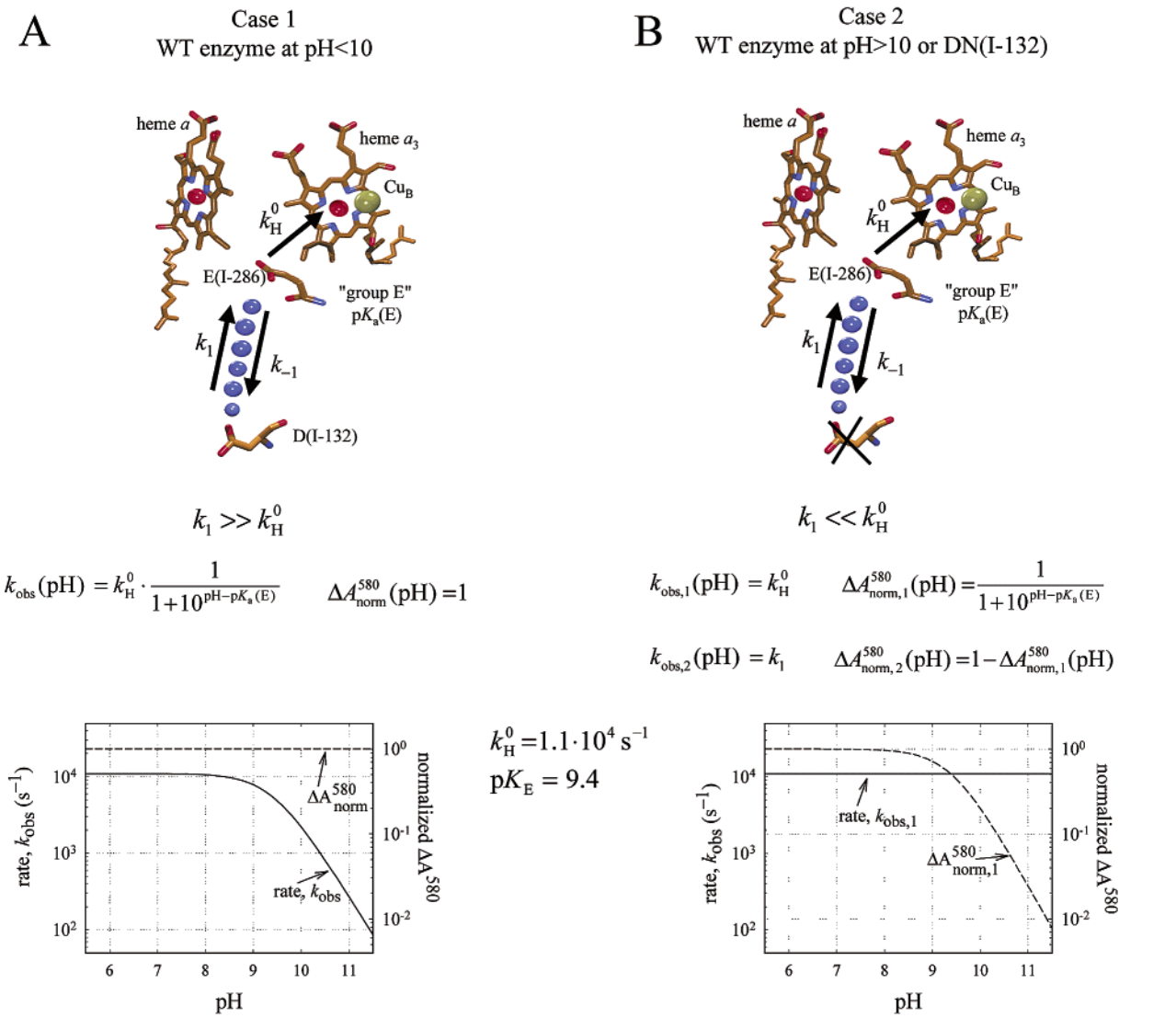

FIGURE 7: A schematic illustration of the two limiting cases 1 and 2 of the model in eq 1. k_{obs} is the observed rate constant of F intermediate formation (increase in absorbance at 580 nm). (A) According to case 1(observed with the wild-type enzyme at pH ≤ 10), the group E (which is assumed to be E(I-286), see Discussion) is in rapid proton equilibrium with the bulk solution so that $k_1 \gg k_H^0$. In this case k_{obs} is described by eq 2b (solid line in the graph in panel A); i.e., the rate is determined by k_H^0 and the fraction protonated E. The amount of F formed is pH-independent, i.e., the normalized $\Delta A^{580}_{norm} = 1$ (dashed line in panel A). (B) According to case 2 (cf. the wild-type enzyme at pH >10 and the DN(I-132) mutant enzyme), the proton-transfer rate from group E to the binuclear center is faster than the proton equilibrium between E and the bulk solution. In this case there are two enzyme populations on the time scale of F intermediate formation. In one population group E, is protonated and F is formed with a rate constant k_H^0. In the other population, E is not protonated. Therefore, formation of F is much slower, determined by proton-transfer all the way from the bulk solution with a rate k_1. The observed rate is biphasic and the amplitudes of these two phases are $\Delta A^{580}_{norm,1}$ and $\Delta A^{580}_{norm,2}$. In practice, the slower of the two phases (with rate k_1) overlaps with the next transition (F → O). Therefore, only one P_R → F phase is seen with rate $k_{obs,1}$ and amplitude at 580 nm, $\Delta A^{580}_{norm,1}$, as shown in the graph.

driving force should be large because the energy must be sufficient to translocate at least one proton across the membrane in the presence of a gradient. The electrochemical gradient across the membrane at physiological conditions is normally ~200 mV, which corresponds to a driving force, ΔpK_a, of ~3 units. This large ΔpK_a is further supported by results from a recent study (Namslauer et al., unpublished data) which indicate that when the apparent pK_a of the proton donor is raised by ~1.5 units (as determined from the pH dependence of the P_R → F kinetics), the F intermediate is still formed to ~100% at pH 11. This implies that in the wild-type enzyme the pK_a of the proton acceptor at the catalytic site must be ≥12 (1 unit difference in the pK_a and the pH on the outside results in F formation in 90% of the enzyme population). A likely proton acceptor at the catalytic site is the hydroxide ion bound to Cu_B in the P_R state (*5*) (see Figure 2B). The pK_a of H_2O is 15.7 in an aqueous solution. Even if it is likely to be lower when the base OH^- is stabilized by binding to a metal ion (*33*), taken into account that the pK_a is expected to depend strongly on the protein environment, a value of ≥12 for the proton acceptor is not unlikely.

Proton Uptake and F Formation above pH 10. As seen in Figure 4A, in the measured pH range above pH 10.3, there is a deviation of the data (P_R → F rate) from the solid line based on the limiting conditions of eq 1 ($k_1 \gg k_H^0$, see case 1 in Figure 7A). This is because proton uptake from the bulk

solution becomes rate-limiting above pH 10; i.e., k_1 is no longer much larger than k_H^0 (cf. Figure 7), and E(I-286) is no longer in rapid equilibrium with the bulk solution on the time scale of F formation. It should be noted that we assume the same model (eq 1) in the entire pH range. The deviation of the solid line from the data in Figure 4A means that the simplification based on the assumption that $k_1 \gg k_H^0$, discussed above, is not valid in the pH range above pH 10.

We note that another limiting case of eq A3 in the Appendix (case 2) is obtained if the equilibrium between the bulk solution and group E (eq 1) is much slower than the proton transfer from E_H to the binuclear center, i.e., $k_1 \ll k_H^0$. In this case there are two enzyme populations that react differently (note that E is assumed to be in equilibrium with the bulk solution prior to the experiment). In one population (α_{EH}, see eq 2c above, given by eq A2) group E is protonated and the observed rate is k_H^0. The normalized amplitude of the absorbance change at 580 nm with the rate $k_{OBS,1} = k_H{}^0$, $\Delta A^{580}_{norm,1}(pH)$, see Figure 7B, is thus

$$\Delta A^{580}_{norm,1}(pH) = \frac{1}{1 + 10^{pH-pK_a(E)}} \quad (3)$$

In the remaining population E is not protonated, and the proton is transferred from the bulk solution with the observed rate $k_{obs,2} = k_1$.

The time dependence of EC_H formation is described by (derived from eq A3):

$$[EC_H](t,pH) \cong 1 - [\alpha_{EH}(pH) \exp(-t \cdot k_H{}^0) + (1 - \alpha_{EH}(pH)) \exp(-t \cdot k_1)] \quad (4)$$

According to case 2, there is one kinetic phase with a rate constant of $k_H{}^0$ (from the enzyme fraction with protonated E, $\alpha_{EH}(pH)$) and one kinetic phase with rate k_1 (in an enzyme fraction 1-$\alpha_{EH}(pH)$). The total amplitude of the two phases is constant, but their relative contribution changes with pH. In the pH range above 10, the latter of the two phases, with rate k_1, dominates. For example, at pH 10.3 the data could be fitted with two rate constants of $k_{obs,1}$ ($k_H{}^0$) = $1.2 \cdot 10^4$ s^{-1}, $k_{obs,2}$ (k_1) = 710 s^{-1}, with a larger contribution from the latter, which is consistent with the model (see "*" and "+" in Figure 4). As indicated above, the total extent of F formed should be constant in the entire pH range. However, at high pH, where the rate is biphasic, the component with the rate $k_{obs,2}$ is the same as that of proton uptake from the bulk solution, which also determines the rate of the next reaction step, the F → O transition (because this transition requires proton uptake from the bulk solution). Thus, in the enzyme fraction with unprotonated group E, 1-$\alpha_{EH}(pH)$, F is not populated to any detectable level and therefore the reaction apparently proceeds directly from P_R to O at high pH. Consequently, the observed amplitude of the absorbance increase at 580 nm ($\Delta A^{580}_{norm,1}(pH) + \Delta A^{580}_{norm,2}(pH)$), associated with formation of F decreases with increasing pH as seen in Figures 3 and 4B.

Proton Uptake from the Bulk Solution to the D-Pathway. We note that, e.g., at pH 9.8 the measured rate of proton uptake from the bulk solution, k_{obs}, is ~$3.1 \cdot 10^3$ s^{-1}. If the proton is taken from the aqueous solution, the proton-uptake rate, k_1, is determined by the second-order rate constant for the diffusion-controlled proton uptake, $k_1{}^0$, and the bulk proton concentration: $k_1{}^0 \cdot [H^+]$. Since at pH 9.8 $k_1 > 3.1 \cdot 10^3 s^{-1}$, we obtain $k_1{}^0 > 2 \cdot 10^{13}$ $M^{-1}s^{-1}$. This simple estimation shows that the proton uptake is much faster than is expected from a diffusion-controlled protonation reaction ($k_H^0 \cong 4 \cdot 10^{10}$ $M^{-1}s^{-1}$, *34*, see also ref *4*). The possibility that the proton is taken directly from the dye (at a concentration of 40 μM) in the solution is excluded since the extent and rate of F formation at pH 10 were exactly the same in a buffer-free solution as with 40 μM dye or 50 mM buffer. Thus, the data indicate that the proton is taken from buffering groups at the surface, in rapid equilibrium with the proton pool in the bulk solution. This type of scenario has been discussed by Gutman and Nachliel, in terms of a "proton-collecting antenna" (*34*, see also ref *35*). Such antenna were suggested to consist of a number of interacting groups, including carboxylates that attract protons through electrostatic interactions and histidine residues that act as a local proton buffer near the entry point of a proton pathway. Similar structures have been found also in other enzymes which show fast rates of proton uptake (*36*).

On the basis of the above discussion, we concluded that proton transfer from the bulk solution to E(I-286), k_1, is much faster than k_H^0 in the pH range up to pH 10 but becomes rate-limiting at pH >10 and, e.g., at pH 10.5 the observed proton-uptake rate is slower than the rate expected from the titration curve based on case 1, Figure 4A. Therefore, if one would plot the true proton uptake rate (k_1) from the bulk solution as a function of pH, the points would be found above the titration curve in Figure 4A at pH <10 but below the curve at pH >10. Thus, the maximum slope of the (hypothetical) trace k_1(pH) corresponds to a decrease in rate that is larger than 1 order of magnitude per pH unit (i.e., a slope of −1 in Figure 4A).

As discussed above, the proton uptake during the P_R → F transition is in this case not a diffusion-controlled reaction, but rather a direct proton transfer from interacting surface groups. Thus, one possible explanation for a slope < −1 is that the protonation of groups near the entry point of the D-pathway is cooperative by way of electrostatic interactions and/or structural rearrangements of the surface groups. However, in this context it should be pointed out that in the above discussion we have assumed that the rate of *internal* proton transfer from E(I-286) to the binuclear center, $k_H{}^0$, is pH-independent. If this is not the case, the deviation of the rate from that predicted from the model (case 1), may be due to a slowing of this internal rate due to, e.g., structural changes around the E(I-286) site at pH >10.

Internal Proton Transfer in the DN(I-132) Mutant Enzyme. To further investigate the mechanism of proton transfer during the P_R → F transition, we studied the reaction as a function of pH in the DN(I-132) mutant enzyme. In this enzyme form, the proton needed to form F is taken internally, presumably from E(I-286), and reprotonation of E(I-286) is blocked. This scenario is consistent with case 2 discussed above (see Figure 7), i.e., $k_1 \ll k_H^0$. With the DN(I-132) enzyme, the protonation state of E prior to the experiment is determined by the pH and pK_a(E). Since the proton equilibrium between the bulk solution and E is much slower than the P_R → F transition, on the time scale of the experiment there are two enzyme populations, one in which

E is protonated and one in which E is not protonated. The fraction in which E is protonated is described by eq 2 and in this fraction F is formed with the same rate ($k_{obs,1} = k_H^0 = 1.1 \cdot 10^4$ s^{-1}) as that at low pH with the wild-type enzyme (where E is fully protonated). In the remaining fraction of the DN(I-132) mutant enzyme, the F formation rate is determined by the proton-uptake rate from the bulk solution ($k_{obs,2} = k_1 \cong 4$ s^{-1}); i.e., it merges with the rate of the F → O transition. The observed decrease in the amplitude of the 580 nm absorbance change with rate k_H^0 in the DN(I-132) mutant enzyme does not exactly follow the pH dependence simulated by eq 2, using the parameters determined with the wild-type enzyme. The apparent pK_a is shifted to a higher value in the mutant enzyme (by ∼1 pH unit).

As seen in Figure 4B, the amplitude of the absorbance increase at 580 nm associated with formation of intermediate F in the DN(I-132) mutant enzyme is about half of that observed with the wild-type enzyme, at pH ≤9.5. In the wild-type enzyme, the P_R → F transition is associated with electron transfer from Cu_A to heme *a*. Thus, since in the DN(I-132) enzyme the electron transfer from Cu_A to heme *a* does not take place, the smaller absorbance change could be due to lack of this electron transfer. According to published data with the bovine enzyme (*37*−*40*) and our unpublished data with the *R. sphaeroides* enzyme, the absorbance change at 580 nm upon reduction of heme *a* (i.e., the reduced minus oxidized difference spectrum) is small. Due to variation of the isosbestic points in different investigations, the spectral contribution has been reported to be either positive (*39*, and unpublished data with the *R. sphaeroides* enzyme) or negative (*37*, *38*, *40*).The assignment of the contribution from heme *a* is further complicated by the fact that these heme *a* redox difference spectra were obtained at equilibrium conditions with enzyme in which the binuclear center was poised in either the reduced or oxidized form with CO or CN^-, respectively. Therefore, these difference spectra might not be directly comparable to the redox difference spectrum of heme *a* in a transient state during enzyme turnover. A more relevant comparison is that with a previously investigated mutant enzyme (ML(II-263)) in which the electron transfer from Cu_A to heme *a* was slowed due to increased midpoint potential of Cu_A. In this enzyme a smaller absorbance increase at 580 nm was seen during the P_R → F transition even though proton uptake from bulk solution was not impaired. Consequently, we propose that the smaller increase at 580 nm in the DN(I-132) than in the wild-type enzyme is due to the lack of electron transfer from Cu_A to heme *a* on the time scale of the P_R → F transition in the former. It should be noted that the intrinsic rate of the internal proton transfer, k_H^0, is the same in the DN(I-132) as that in the wild-type enzyme.

As seen in Figure 6, a decrease in absorbance at 580 nm with a time constant of ∼4 ms was observed after formation of F. The cause of this absorbance decrease is unclear.

The Properties of E(I-286). Results from experiments using Fourier transform infrared (FTIR) spectroscopy on cytochrome *c* oxidase from *P. denitrificans* and bovine heart and ubiquinol oxidase from *E. coli* (*32*, *41*−*44*) indicated that E(I-286) (*R. sphaeroides* numbering) has an unusually high pK_a compared to the solution value and that it is at least partly protonated up to pH 10, which is consistent with the pK_a of 9.4, determined in this study. However, it should be noted that in the FTIR experiments as well as in theoretical calculations, a static pK_a in a specific state is determined. In the experiments discussed in the present study, an apparent pK_a is determined from the kinetics. This apparent pK_a may reflect the pK_a of the proton donor in a transient conformation from which it donates a proton. Moreover, the measured value of the pK_a may also include the equilibrium constant between the two conformations of the proton donor.

The structure of the *R. sphaeroides* cytochrome *c* oxidase shows that E(I-286) is connected with the protein surface through a chain of water molecules and polar amino acid residues over a distance of ∼24 Å. From E(I-286) the structural properties of the proton pathway are less clear. Between E(I-286) and the binuclear center there is a hydrophobic cavity, which most likely contains water molecules that conduct protons. To transfer a proton the side chain of E(I-286) may have to move toward the binuclear center (*45*−*48*). The results from this study show that the proton-transfer rate from E(I-286) to the binuclear center, k_H^0, is $1.1 \cdot 10^4$ s^{-1}. This rate may reflect the proton transfer through the hydrophobic cavity. However, it may also be determined by the dynamics of the E(I-286) side chain (see (*49*)) and the transfer of pumped protons (see below).

Relatively high pK_a values of functionally important carboxylates have also been found in other biological systems. For example, in bacteriorhodopsin, the light-induced proton-transfer involves an internal proton transfer from Asp 96 to the Schiff base. The aspartate is located in a hydrophobic environment, connected through a proton pathway to the cytoplasmic surface. It was found to have a pK_a of >11 in the ground state, but its affinity for protons is lowered in the transition where the proton is donated (for review, see (*50*)).

The D-pathway in cytochrome *c* oxidase is used for the transfer of both substrate and pumped protons during reaction of the reduced enzyme with O_2. This means that there must be a branching point at which the substrate protons are transferred to the catalytic site and the pumped protons to an acceptor, in contact with the output side of the enzyme. To prevent the transfer of all protons to O_2, proton-transfer reactions from this point must be regulated either by controlling the rates and/or driving forces to the acceptor of pumped protons and the catalytic site, respectively. Even though the experiments discussed here were done with the solubilized enzyme and only the net proton uptake is observed, the enzyme presumably pumps protons during the P_R → F transition. Since both pumped and substrate protons are transferred through the D-pathway, proton pumping requires that the transfer of the proton to be pumped is tightly coupled to the transfer of the substrate proton to the catalytic site. Therefore, the rate-limiting step for the proton transfer to the catalytic site upon formation of intermediate F may be determined by the transfer of a "pumped proton". If this is the case, the pK_a and proton-transfer rate, k_H^0, that were determined from this study may reflect those for the transfer of a proton from E(I-286) to an acceptor for pumped protons.

CONCLUSIONS

The examination of the pH dependence of the rates and amplitudes of the P_R → F transition and the proton uptake

from the bulk solution associated with the reaction made it possible to determine an apparent pK_a value of E(I-286) of 9.4. The proton-transfer rate from E(I-286) to a proton acceptor was found to be $1.1 \cdot 10^4$ s^{-1}. Reprotonation of E(I-286) from the bulk solution was found to be at least a factor of 100 faster than that expected from a diffusion-controlled reaction, which shows that surface groups around the entry point of the D-pathway provide a local surface-bound buffer that facilitates the proton uptake. This work establishes the foundation for future and ongoing work on mutant forms of cytochrome *c* oxidase in which the thermodynamic properties of the D-pathway are altered. For example, the pK_a of E(I-286) could be modified in a controlled way making it possible to investigate the proton-transfer rate as a function of driving force, as has been done previously with carbonic anhydrase (*51*).

ACKNOWLEDGMENT

The authors thank Pia Ädelroth and Alexei Stuchebrukhov for valuable insights and Ida Holmgren for excellent technical assistance.

APPENDIX

Model. The model in eq A1 is used as a framework for a discussion of the experimental data (see Figure 7):

$$(\text{bulk}) \underset{k_{-1}}{\overset{k_1}{\rightleftharpoons}} E_HC \xrightarrow{k_H^0} EC_H \qquad \text{(A1)}$$

In the model E is a protonatable group in the D-pathway, assumed to be E(I-286) (see Discussion), C is the binuclear center, and "bulk" is the bulk solution; or alternatively, it could be a protonatable group at the protein surface that is in rapid equilibrium with the bulk solution (see Discussion). The subscript H indicates a protonated site. Here C and C_H correspond to states P_R and F, respectively, at the binuclear center. We assume that the group E is in equilibrium with the bulk solution before the proton-transfer reaction (i.e., before initiation of the experiment), independently of the values of k_1 and k_{-1}. This means that the concentration of state E_HC, normalized to the total enzyme concentration, at $t = 0$, $[E_HC](0)$, is

$$[E_HC](0) = \frac{k_1}{k_1 + k_{-1}} = \frac{k_1^0 \cdot [H^+]}{k_1^0 \cdot [H^+] + k_{-1}} = \frac{1}{1 + 10^{pH - pK_a(E)}} \qquad \text{(A2)}$$

where $[H^+]$ is the proton concentration in the bulk solution, k_1° is the second-order rate constant for proton transfer from solution to the protein, and the acidification constant of group E is $K_a(E) = k_1^0/k_{-1}$. The proton transfer from E_H to the binuclear center is assumed to be irreversible as discussed in the Discussion section.

With cytochrome *c* oxidase, there are two experimental observables: (i) the absorbance increase at 580 nm, which reflects the formation of state F from state P_R at the binuclear center, i.e., $\Delta A^{580}(t) = \Delta A_0^{580} \cdot [EC_H](t)$, where ΔA_0^{580} is the absorbance change at 580 nm associated with the $P_R \rightarrow F$ transition in 100% of the enzyme population, and (ii) proton uptake from the bulk solution, i.e., changes in the bulk pH are monitored.

The expressions for the two concentrations, normalized to the total enzyme concentration, are

$$[EC_H](t) = \frac{k_1 k_H^0}{\kappa_1 \kappa_2} - \frac{k_H^0 (k_1 - [E_HC](0)\kappa_1)}{\kappa_1(\kappa_2 - \kappa_1)} \exp(-\kappa_1 t) - \frac{k_H^0 (k_1 - [E_HC](0)\kappa_2)}{\kappa_2(\kappa_1 - \kappa_2)} \exp(-\kappa_2 t) \qquad \text{(A3)}$$

where κ_1 and κ_2 are solutions to eq A4 taken with the reverse signs:

$$\kappa^2 + (k_1 + k_{-1} + k_H^0) \cdot \kappa + k_1 \cdot k_H^0 = 0 \qquad \text{(A4)}$$

REFERENCES

1. Malmström, B. G. (1990) *Chem. Rev. 90*, 1247−1260.
2. Knowles, J. R. (1976) *CRC Crit. Rev. Biochem. 4*, 165−173.
3. Oliveberg, M., Brzezinski, P., and Malmström, B. G. (1989) *Biochim. Biophys. Acta 977*, 322−328.
4. Hallén, S., and Nilsson, T. (1992) *Biochemistry 31*, 11853−11859.
5. Zaslavsky, D., and Gennis, R. B. (2000) *Biochim. Biophys. Acta 1458*, 164−179.
6. Ferguson-Miller, S., and Babcock, G. T. (1996) *Chem. Rev. 96*, 2889−2907.
7. Babcock, G. T., and Wikström, M. (1992) *Nature 356*, 301−309.
8. Einarsdóttir, Ó. (1995) *Biochim. Biophys. Acta 1229*, 129−147.
9. Ädelroth, P., Ek, M., and Brzezinski, P. (1998) *Biochim. Biophys. Acta 1367*, 107−117.
10. Morgan, J. E., Verkhovsky, M. I., Palmer, G., and Wikström, M. (2001) *Biochemistry 40*, 6882−6892.
11. Babcock, G. T. (1999) *Proc. Natl. Acad. Sci. U.S.A. 96*, 12971−12973.
12. Karpefors, M., Ädelroth, P., Namslauer, A., Zhen, Y. J., and Brzezinski, P. (2000) *Biochemistry 39*, 14664−14669.
13. Oliveberg, M., Hallén, S., and Nilsson, T. (1991) *Biochemistry 30*, 436−440.
14. Hill, B. C. (1991) *J. Biol. Chem. 266*, 2219−2226.
15. Karpefors, M., Ädelroth, P., Zhen, Y., Ferguson-Miller, S., and Brzezinski, P. (1998) *Proc. Natl. Acad. Sci. U.S.A. 95*, 13606−13611.
16. Siletsky, S., Kaulen, A. D., and Konstantinov, A. A. (1999) *Biochemistry 38*, 4853−4861.
17. Ädelroth, P., Karpefors, M., Gilderson, G., Tomson, F. L., Gennis, R. B., and Brzezinski, P. (2000) *Biochim. Biophys. Acta 1459*, 533−539.
18. Smirnova, I. A., Ädelroth, P., Gennis, R. B., and Brzezinski, P. (1999) *Biochemistry 38*, 6826−6833.
19. Aagaard, A., Namslauer, A., and Brzezinski, P. (2002) *Biochim. Biophys. Acta 1555*, 133−139.
20. Konstantinov, A. A., Siletsky, S., Mitchell, D., Kaulen, A., and Gennis, R. B. (1997) *Proc. Natl. Acad. Sci. U.S.A. 94*, 9085−9090.
21. Rich, P. R., Jünemann, S., and Meunier, B. (1998) *J. Bioenerg. Biomembr. 30*, 131−138.
22. Zhen, Y. (1998) Ph.D. Thesis, Michigan State University, East Lansing, MI.
23. Mitchell, D. M., and Gennis, R. B. (1995) *FEBS Lett. 368*, 148−150.
24. Fetter, J. R., Qian, J., Shapleigh, J., Thomas, J. W., García-Horsman, A., Schmidt, E., Hosler, J., Babcock, G. T., Gennis, R. B., and Ferguson-Miller, S. (1995) *Proc. Natl. Acad. Sci. U.S.A. 92*, 1604−1608.
25. Brändén, M., Sigurdson, H., Namslauer, A., Gennis, R. B., Ädelroth, P., and Brzezinski, P. (2001) *Proc. Natl. Acad. Sci. U.S.A. 98*, 5013−5018.
26. Ädelroth, P., Svensson Ek, M., Mitchell, D. M., Gennis, R. B., and Brzezinski, P. (1997) *Biochemistry 36*, 13824−13829.
27. Watmough, N. J., Katsonouri, A., Little, R. H., Osborne, J. P., Furlong-Nickels, E., Gennis, R. B., Brittain, T., and Greenwood, C. (1997) *Biochemistry 36*, 13736−13742.

28. Verkhovskaya, M. L., García-Horsman, A., Puustinen, A., Rigaud, J. L., Morgan, J. E., Verkhovsky, M. I., and Wikström, M. (1997) *Proc. Natl. Acad. Sci. U.S.A. 94*, 10128−10131.
29. Mills, D. A., Schmidt, B., Hiser, C., Westley, E., and Ferguson-Miller, S. (2002) *J. Biol. Chem. 277*, 14894−14901.
30. Gilderson, G., Aagaard, A., and Brzezinski, P. (2002) *Biophys. Chem. 98*, 105−114.
31. Kannt, A., Roy, C., Lancaster, D., and Michel, H. (1998) *Biophys. J. 74*, 708−721.
32. Rich, P. R., Breton, J., Jünemann, S., and Heathcote, P. (2000) *Biochim. Biophys. Acta 1459*, 475−480.
33. Lippard, S. J., and J. M., B. (1994) *Principles of Bioinorganic Chemistry*, University Science Books, Mill Valley, CA.
34. Gutman, M., and Nachliel, E. (1990) *Biochim. Biophys. Acta 1015*, 391−414.
35. Georgievskii, Y., Medvedev, E. S., and Stuchebrukhov, A. A. (2002) *Biophys. J. 82*, 2833−2846.
36. Ädelroth, P., Paddock, M. L., Sagle, L. B., Feher, G., and Okamura, M. Y. (2000) *Proc. Natl. Acad. Sci. U.S.A. 97*, 13086−13091.
37. Moody, A. J., and Rich, P. R. (1990) *Biochim. Biophys. Acta 1015*, 205−215.
38. Ellis, W. R., Jr., Wang, H., Blair, D. F., Gray, H. B., and Chan, S. I. (1986) *Biochemistry 25*, 161−167.
39. Vanneste, W. H. (1966) *Biochemistry 5*, 838−848.
40. Liao, G. L., and Palmer, G. (1996) *Biochim. Biophys. Acta 1274*, 109−111.
41. Puustinen, A., Bailey, J. A., Dyer, R. B., Mecklenburg, S. L., Wikström, M., and Woodruff, W. H. (1997) *Biochemistry 36*, 13195−13200.
42. Lübben, M., Prutsch, A., Mamat, B., and Gerwert, K. (1999) *Biochemistry 38*, 2048−2056.
43. Heitbrink, D., Sigurdson, H., Bolwien, C., Brzezinski, P., and Heberle, J. (2002) *Biophys. J. 82*, 1−10.
44. Hellwig, P., Rost, B., Kaiser, U., Ostermeier, C., Michel, H., and Mäntele, W. (1996) *FEBS Lett. 385*, 53−57.
45. Riistama, S., Hummer, G., Puustinen, A., Dyer, R. B., Woodruff, W. H., and Wikström, M. (1997) *FEBS Lett 414*, 275−280.
46. Hofacker, I., and Schulten, K. (1998) *Proteins 30*, 100−107.
47. Iwata, S., Ostermeier, C., Ludwig, B., and Michel, H. (1995) *Nature 376*, 660−669.
48. Svensson-Ek, M., Abramson, J., Larsson, G., Törnroth, S., Brzezinski, P., and Iwata, S. (2002) *J. Mol. Biol. 321*, 329−339.
49. Karpefors, M., Ädelroth, P., and Brzezinski, P. (2000) *Biochemistry 39*, 6850−6856.
50. Balashov, S. P. (2000) *Biochim. Biophys. Acta 1460*, 75−94.
51. Silverman, D. N. (2000) *Biochim. Biophys. Acta 1458*, 88−103.
52. Humphrey, W., Dalke, A., and Schulten, K. (1996) *J. Mol. Graph. 14*, 33.

BI026524O